Surface & Coatings Technology 279 (2015) 166–170

Contents lists available at ScienceDirect

Surface & Coatings Technology

journal homepage: www.elsevier.com/locate/surfcoat

Effects of silver plasma immersion ion implantation on the surface characteristics and cytocompatibility of titanium nitride films

Ruizhen Xu [a,b], Xiongbo Yang [a,*], Jiang Jiang [b,c], Penghui Li [b], Xuming Zhang [b], Guosong Wu [b], Paul K. Chu [b,*]

[a] College of Science, China Three Gorges University, Yichang 443002, China
[b] Department of Physics and Materials Science, City University of Hong Kong, Tat Chee Avenue, Kowloon, Hong Kong, China
[c] Institute of Technical Biology and Agricultural Engineering, Chinese Academy of Sciences, Hefei 230031, China

ARTICLE INFO

Article history:
Received 26 June 2015
Revised 3 August 2015
Accepted in revised form 15 August 2015
Available online 22 August 2015

Keywords:
TiN
Silver
Plasma immersion ion implantation
Cytocompatibility

ABSTRACT

Titanium nitride (TiN) coatings are commonly used on surgical instruments for its suitable hardness as well as excellent chemical inertness properties. Silver (Ag), as an antibacterial agent, is implanted into TiN films by plasma immersion ion implantation (PIII). The changes in the surface characteristics are investigated and rat calvaria osteoblasts are cultured to evaluate the cytocompatibility. The results indicate that Ag PIII samples implanted with small amounts of Ag have good cytocompatibility while the desirable surface properties are preserved.

1. Introduction

Owing to their high abrasion-resistant properties, transition metal nitrides are widely used as protective coatings in industrial applications. Titanium nitride (TiN), a representative transition metal nitride, has the extraordinary combination of desirable physical, chemical, and mechanical characteristics [1–6]. These remarkable characteristics such as high hardness (~20–22 GPa) [7] and chemical inertness make it attractive in applications such as orthopedic prostheses, cardiac valves, and joint arthroplasty [8–11]. After surgical insertion, infection is one of the serious complications and may be difficult to treat sometimes requiring removal [12]. Hence, it is crucial to endow the materials with the long-term ability to combat bacterial colonization to allow smooth healing. Silver (Ag) is an effective antibacterial agent capable of killing antibiotic-resistant bacteria and it shows no local or systemic side-effect in many *in vivo* experiments [13]. Wan et al. reported that the antibacterial activity of the silver implanted sample against *Staphylococcus aureus* was improved [14]. To achieve low cytotoxicity, Zhao et al. suggested that the silver release rate needed to be controlled [15]. Since the required Ag dose is typically low but long-term Ag release is required, plasma immersion ion implantation (PIII) is the an excellent technique to introduce the suitable amount of Ag to a predesigned depth to facilitate controlled long-term release while the favorable bulk attributes of the materials are not compromised [16,17]. Nonetheless, although the antimicrobial effects of Ag are proven, the cytocompatibility of the plasma-implanted materials is another important issue that needs attention. In this work, Ag is introduced into TiN films by PIII and the surface mechanical and cytocompatibility are studied.

2. Materials and methods

TiN films were prepared on silicon wafers by magnetron sputtering at a pressure of 10^{-4} Pa. After pre-cleaning by argon sputtering, an

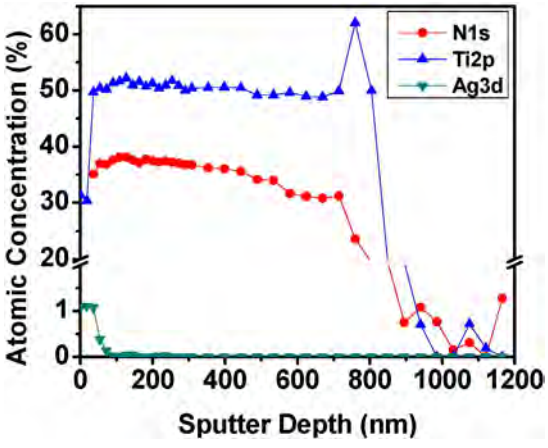

Fig. 1. XPS depth profiles acquired from the Ag-PIII TiN film.

* Corresponding authors.
E-mail addresses: shiheren@hotmail.com (X. Yang), paul.chu@cityu.edu.hk (P.K. Chu).

http://dx.doi.org/10.1016/j.surfcoat.2015.08.033
0257-8972/

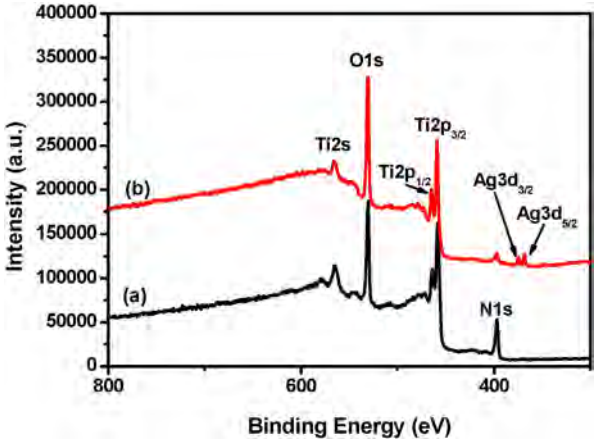

Fig. 2. XPS survey spectra of (a) TiN and (b) Ag-PIII.

intermediate Ti layer was deposited at room temperature using a high purity (99.99%) Ti target at an argon flow rate of 20 sccm and 250 W sputtering power for 5 min. Afterwards, TiN films were deposited in a gas mixture comprising Ar (10 sccm) and nitrogen (4 sccm) at the same sputtering power for 4 h. Finally, silver was introduced into the TiN film by plasma immersion ion implanted (PIII). The silver plasma was generated from a pure silver cathode (99.99%) using a repetition frequency of 10 Hz, pulse duration of 400 μs, and pulsed voltage of 25 kV. PIII was under a pressure of 10^{-4} Pa and conducted for 3 h.

The depth profiles were determined by X-ray photoelectron spectroscopy (XPS, Physical Electronics PHI 5802). Al K_α irradiation was employed and the estimated sputtering rates were 8 nm/min in the first 17 min and 45 nm/min afterwards based on standards sputtered under similar conditions. Field-emission scanning electron microscopy (FE-SEM, FEI/Philips XL30 Esem-FEG) was conducted to examine the morphology of the surface before and after PIII. The hydrophilicity of the surface was determined by static contact angle measurements using distilled water as the medium on a Rame-Hart (USA) instrument at room temperature. To evaluate the hardness of the TiN film before and after Ag PIII, an MTS nano-indenter was utilized.

The sample was cut into 1 cm × 1 cm for cell culturing. The MC3T3-E1 cells were cultured in a Dulbecco's Modified Eagle Medium (DMEM, GIBCO, cat. no. 12100-046) supplemented with 10% fetal bovine serum (FBS, GIBCO, cat. no. 10270-106). The osteoblasts were seeded at a density of 3×10^4 cells per well on 24-well tissue culture plates and incubated in a humidified atmosphere of 5% CO_2 at 37 °C. The morphology of the cells was examined by double fluorescence staining. After incubation for 24 h, the osteoblasts were fixed with 2% paraformaldehyde and immunofluorescently stained with the cytoskeleton protein f-actin with phalloidinfluorescein isothiocyanate (Sigma). After the nuclei were counter-stained with 4′,6′-diaidino-2-phenylindole (DAPI), pictures were taken on a digital camera (Carl Zeiss Axio Observer Z1). The cell counting kit-8 (CCK-8 Sigma) was employed to quantitatively evaluate the cell viability. After culturing for 5 h, 1 day, and 3 days, the samples were rinsed twice with sterile PBS to remove weakly attached and unattached cells. They were transferred to 24-well tissue culture plates with a culture medium of 10% CCK-8. After culturing for 4 h, the optical density (OD) was measured at 450 nm on a power wave microplate spectrophotometer (BioTek, USA). The statistical analysis was performed based on the one-way ANOVA analysis.

3. Results and discussion

Fig. 1 shows the elemental depth profiles of the Ag-PIII TiN film. The maximum Ti concentration of 62% is found at a depth of about 760 nm and the nitrogen concentration is over 30% up to a depth of 700 nm. The atomic concentration of Ag is about 1% up to a depth of about 50 nm. Hence, the thickness of the TiN film is approximately 700 nm and the presence of Ag is confirmed.

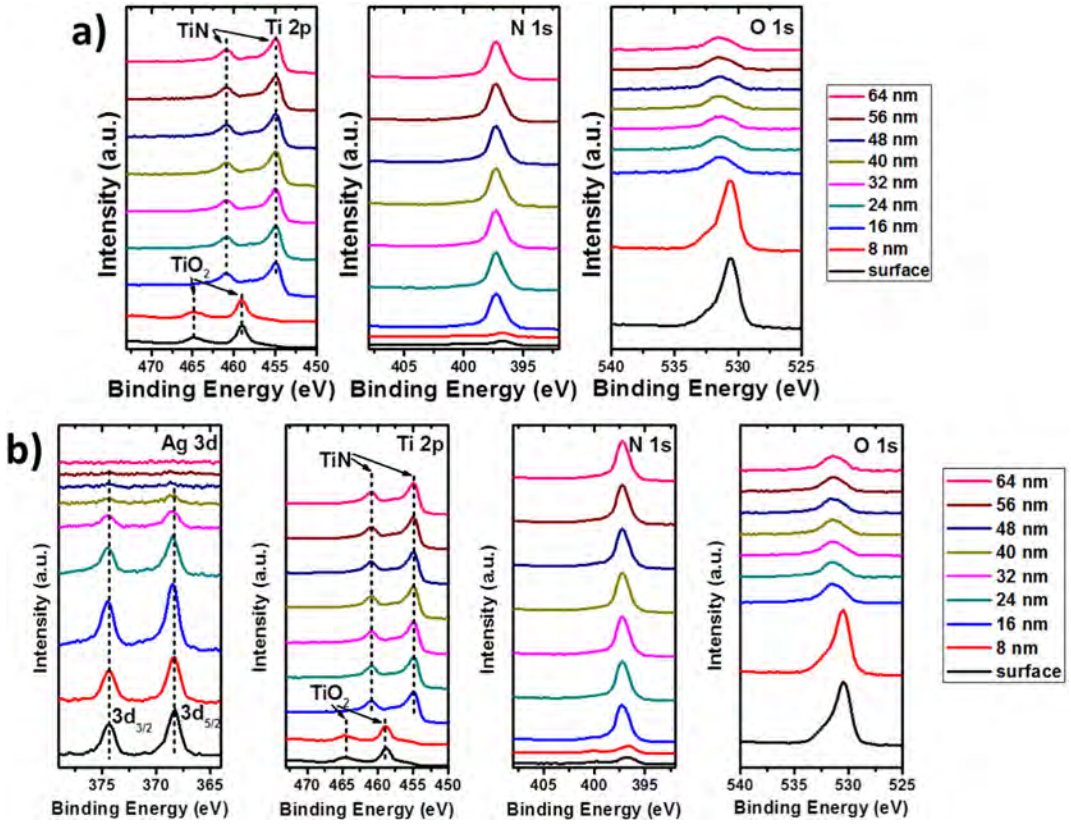

Fig. 3. High-resolution XPS spectra of Ag, Ti, N and O: (a) TiN, and (b) Ag-PIII.

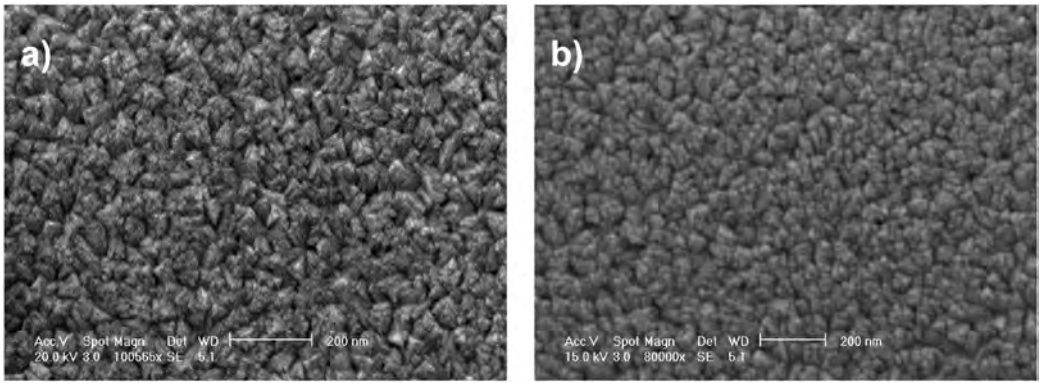

Fig. 4. Surface morphology of the TiN film: (a) control and (b) after Ag-PIII.

To reveal the chemical composition, XPS survey spectra of TiN and Ag-PIII TiN film are display by Fig. 2a and b respectively. The spectrum of TiN sample is dominated by the Ti2p signal at 459 eV as well as O1s signal at 513 eV, and two small peaks due to Ti2s at 566 eV and N1s at 397 eV. The oxygen signal may originate from different sources, including surface contamination, partial oxidation of the surface during storage and handling. It indicates that main product in the surface of the TiN film is titanium oxide. After Ag-PIII, a new signal of Ag3d at 369 eV is observed, which reconfirmed the existent of the Ag element.

The high-resolution XPS spectrum of Fig. 3 is used to determine the nature of the chemical bonding associated with transformation on the surface of TiN film before and after Ag plasma treatment [2,3,18]. Fig. 3a presents the high-resolution XPS spectra of Ti2p, N1s and O1s from the TiN film. With sputtering, the Ti2p peak shifts from the TiO_2 in the near surface to TiN. The data disclose that an oxide layer is present on top of the TiN film. After Ag-PIII, the film is composed of three layers. The outermost layer (within 10 nm) is consisted of Ag and TiO_2, the interlayer (to the depth of around 50 nm) is a mixture of Ag and TiN, and the substrate is TiN film. The results are consistent with the data as observed in Figs. 1 and 2.

The SEM images acquired from the TiN films before and after Ag PIII are depicted in Fig. 4. As shown in Fig. 4a, the surface of the control sample is composed of uniformly-distributed and hill-shaped particles with a size of approximately 40 nm. After Ag PIII (Fig. 4b), many smaller particles with dome-tops are observed from the surface due to energetic bombardment by Ag ions [19].

Fig. 5 shows the water contact angles on the TiN and Ag-PIII films. The contact angles on the samples before and after Ag-PIII are $101.6 \pm 1.2°$ and $99.7 \pm 4.0°$, respectively. Each data point represents the average of five measurements conducted on different parts of each specimen for statistical accountability. The results indicate that the samples are hydrophobic (contact angle larger than 90°) and the Ag PIII sample shows slightly enhanced hydrophilic properties (smaller contact angle). Shibuichi et al. reported that the hydrophobic characteristics were enhanced when the surface roughness increased [20]. Our results reveal similar surface morphologies before and after Ag PIII and consequently similar hydrophilicity.

The load–displacement curves and hardness values are shown in Fig. 6. The load–displacement curves of the control and Ag-PIII samples are almost the same and the hardness values of the TiN film before and after Ag-PIII are 20.5 GPa and 20.1 GPa, respectively. The reproducibility of the nanoindentation measurements is determined by repeating the tests four times and the error bar represents one standard deviation. There is no significant difference in the hardness of the samples before and after PIII. A surface with high hardness property presents more abrasion resistance which bodes well for biomedical applications such as joint arthroplasty [9]. According to XPS, the relatively small Ag concentration does not affect the hardness of the TiN films.

Fig. 7 displays the double-stained osteoblast morphology on the Ag-PIII and TiN sample after culturing for 1 day as observed by fluorescent microscopy at different magnifications. The blue spots stand for the nuclei of the attached cells and green parts are microtubules. Fig. 7a reveals that the overall surface areas of Ag-PIII sample are covered by osteoblasts and Fig. 7b is the magnified figure showing most of membranes flattened spreading and morphology of the osteoblasts. Fig. 7c displays that the surface of TiN is partly covered by osteoblasts and the magnified figure, Fig. 7d, shows most osteoblasts do not spread well even if they adhere on TiN sample. The surface of Ag-PIII is fully covered by cells indicating that it is suitable for osteoblast adhesion. Moreover, many osteoblasts on the Ag-PIII sample have the flattened membranes with an irregular polygonal shape indicative of effective osteoblast attachment and spreading.

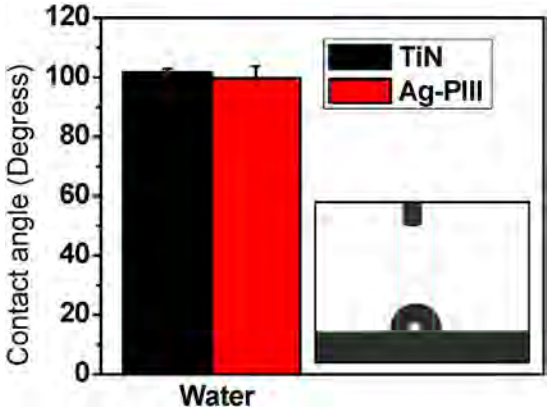

Fig. 5. Water contact angles with the inset at the lower right corner being the representative water droplet image (side-view) on the Ag-PIII sample.

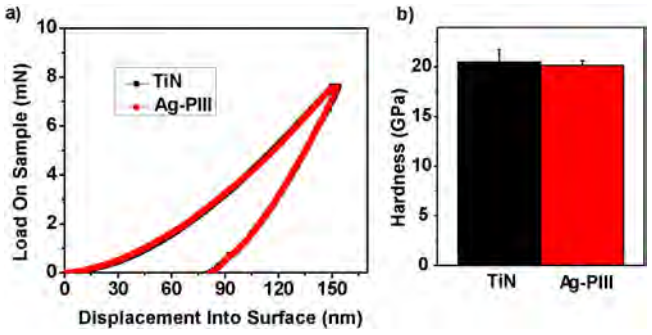

Fig. 6. (a) Load on the sample as a function of displacement into surface and (b) hardness of TiN and Ag-PIII specimens.

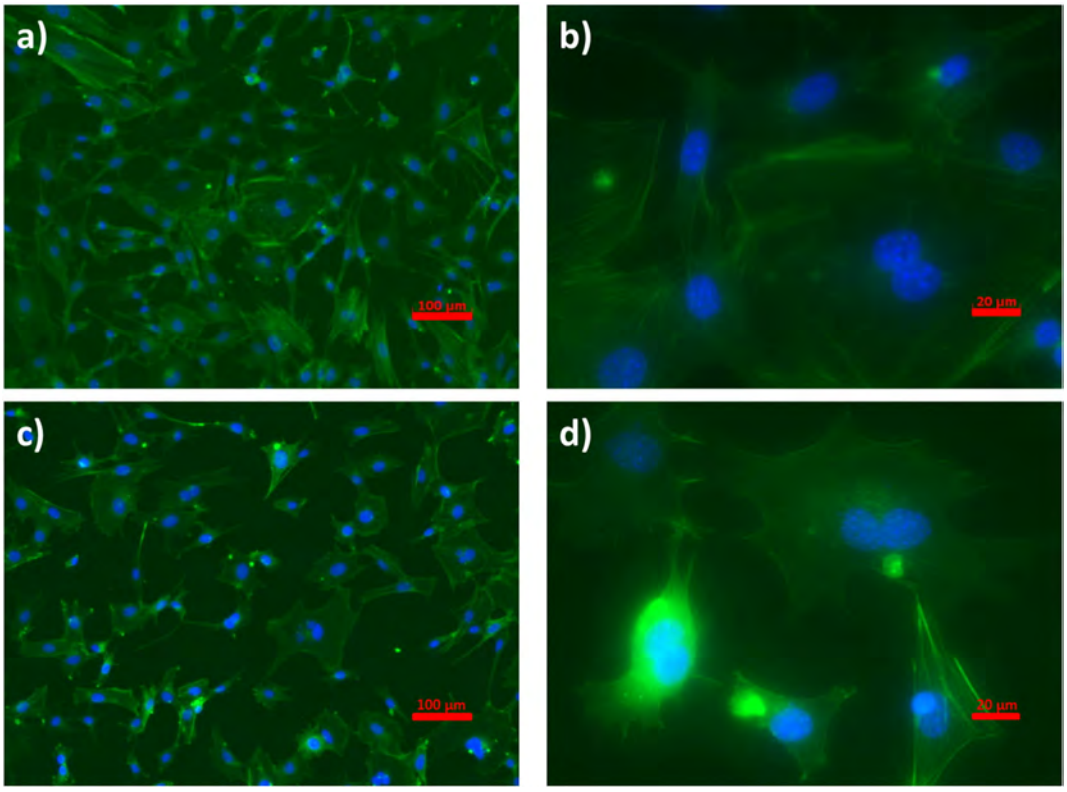

Fig. 7. Morphology of attached MC3T3-E1 cells after 24 h. (a) Ag-PIII sample, (b) magnified image of Ag-PIII sample, (c) TiN sample, and (d) magnified image of TiN sample.

Fig. 8 displays the osteoblasts viability after culturing for 5 h, 1 day, and 3 days. The OD value on the Ag-PIII sample is higher than that on the untreated sample at each time point, suggesting improved osteoblast attachment and growth throughout the period. The interactions between cells and materials affect cell attachment and spreading and influence the subsequent cell performance [21]. The higher quantities of osteoblasts on the Ag-PIII sample are believed to arise from the good adhesion ability which results in a higher degree of cell proliferation [22]. In this study, the good behavior of osteoblasts reveals the cytocompatibility of TiN plasma-implanted with the proper fluence of Ag. Hence, PIII is a safe technique to introduce Ag into TiN films and other material systems to obtain good surface cytocompatibility and antimicrobial properties while the desirable bulk properties of the materials are preserved.

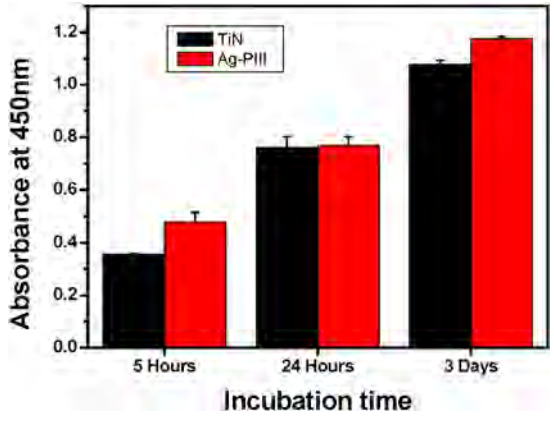

Fig. 8. Cell viability assay of rat calvaria osteoblasts cultured on the TiN and Ag-PIII samples for 5 h, 24 h, and 3 days.

4. Conclusion

Ag is introduced into TiN films by plasma immersion ion implantation and the surface properties and cytocompatibility are studied. After Ag PIII, many fine TiN particles are observed from the surface and the hydrophilic properties are improved slightly although it is still considered hydrophobic. The hardness of the TiN film is about 20 GPa and does not change significantly in spite of the Ag PIII treatment. The osteoblasts seeded on the treated sample exhibit a polygonal shape and cover a large area. The good cell attachment observed from the Ag-PIII sample promotes better cell proliferation compared to the control sample. Our results indicate that the Ag-PIII TiN film not only has good cytocompatibility, but also retains the excellent hardness property.

Acknowledgments

The work was financially supported by the Hong Kong Research Grants Council (RGC) General Research Funds (GRF) No. CityU 112212, City University of Hong Kong Applied Research Grant (ARG) No. 9667085, City University of Hong Kong Strategic Research Grant (SRG) No. 7004188, China Three Gorges University Talent Start-up Funds Nos. KJ2014B079 and KJ2014B080, Key Scientific Research Project of Hubei Provincial Department of Education of China No. D20151205.

References

[1] G. Zeb, P. Viel, S. Palacin, X.T. Le, On the chemical grafting of titanium nitride by diazonium chemistry, RSC Adv. 5 (2015) 50298–50305.
[2] E. Yousefi, M. Ghorbani, A. Dolati, H. Yashiro, M. Outokesh, Preparation of new titanium nitride-carbon nanocomposites in supercritical benzene and their oxygen reduction activity in alkaline medium, Electrochim. Acta 164 (2015) 114–124.
[3] N. Pliatsikas, A. Siozios, S. Kassavetis, G. Vourlias, P. Patsalas, Optical properties of nanostructured Al-rich Al-1 (−) xTixN films, Surf. Coat. Technol. 257 (2014) 63–69.

[4] E. Zalnezhad, A.A.D. Sarhan, M. Hamdi, Investigating the fretting fatigue life of thin film titanium nitride coated aerospace Al7075–T6 alloy, Mater. Sci. Eng., A 559 (2013) 436–446.
[5] C.N. Kirchner, K.H. Hallmeier, R. Szargan, T. Raschke, C. Radehaus, G. Wittstock, Evaluation of thin film titanium nitride electrodes for electroanalytical applications, Electroanal 19 (2007) 1023–1031.
[6] R. Bavadi, S. Valedbagi, Physical properties of titanium nitride thin film prepared by DC magnetron sputtering, Mater. Phys. Mech. 15 (2012) 167–172.
[7] G. Ben-Hamu, A. Eliezer, E.M. Gutman, Electrochemical behavior of magnesium alloys strained in buffer solutions (retraction of vol 52, pg 304, 2006), Electrochim. Acta 52 (2007) 6395.
[8] I. Dion, F. Rouais, L. Triut, C. Baquey, J.R. Monties, P. Havlik, TiN coating: surface characterization and haemocompatibility, Biomaterials 14 (1993) 169–176.
[9] M.J. Pappas, G. Makris, F.F. Buechel, Titanium nitride ceramic film against polyethylene. A 48 million cycle wear test, Clin. Orthop. Relat. Res. 317 (1995) 64–70.
[10] M.T. Raimondi, R. Pietrabissa, The *in-vivo* wear performance of prosthetic femoral heads with titanium nitride coating, Biomaterial 21 (2000) 907–913.
[11] K.H. Chung, G.T. Liu, J.G. Duh, J.H. Wang, Biocompatibility of a titanium–aluminum nitride film coating on a dental alloy, Surf. Coat. Technol. 188 (2004) 745–749.
[12] L.J. Zhang, J.J. Fan, Z. Zhang, F.H. Cao, J.Q. Zhang, C.N. Cao, Study on the anodic film formation process of AZ91D magnesium alloy, Electrochim. Acta 52 (2007) 5325–5333.
[13] H.P. Duan, C.W. Yan, F.H. Wang, Growth process of plasma electrolytic oxidation films formed on magnesium alloy AZ91D in silicate solution, Electrochim. Acta 52 (2007) 5002–5009.
[14] Y.Z. Wan, S. Raman, F. He, Y. Huang, Surface modification of medical metals by ion implantation of silver and copper, Vacuum. 81 (2007) 1114.
[15] L.Z. Zhao, H.R. Wang, K.F. Huo, L.Y. Cui, W.R. Zhang, H.W. Ni, Y.M. Zhang, Z.F. Wu, P.K. Chu, Antibacterial nano-structured titania coating incorporated with silver nanoparticles, Biomaterials 32 (2011) 5706–5716.
[16] P.K. Chu, Surface engineering and modification of biomaterials, Thin Solid Films 528 (2013) 93–105.
[17] P.K. Chu, B.Y. Tang, Y.C. Cheng, P.K. Ko, Principles and characteristics of a new generation plasma immersion ion implanter, Rev. Sci. Instrum. 68 (1997) 1866–1874.
[18] H.H. Elsentriecy, H.M. Luo, H.M. Meyer, L.L. Grado, J. Qu, Effects of pretreatment and process temperature of a conversion coating produced by an aprotic ammonium-phosphate ionic liquid on magnesium corrosion protection, Electrochim. Acta 123 (2014) 58–65.
[19] X.M. Liu, S.L. Wu, P.K. Chu, C.Y. Chung, C.L. Chu, Y.L. Chan, K.W.K. Yeung, W.W. Lu, K.M.C. Cheung, K.D.K. Luk, *In vitro* corrosion behavior of TiN layer produced on orthopedic nickel–titanium shape memory alloy by nitrogen plasma immersion ion implantation using different frequencies, Surf. Coat. Technol. 202 (2008) 2463–2466.
[220] S. Shibuichi, T. Onda, N. Satoh, K. Tsujii, Super water-repellent surfaces resulting from fractal structure, J. Phys. Chem. 100 (1996) 19512–19517.
[21] H. Wang, J. Ji, W. Zhang, W. Wang, Y. Zhang, Z. Wu, P.K. Chu, Rat calvaria osteoblast behavior and antibacterial properties of O(2) and N(2) plasma-implanted biodegradable poly(butylene succinate), Acta Biomater. 6 (2010) 154–159.
[22] X.M. Liu, S.L. Wu, Y.L. Chan, P.K. Chu, C.Y. Chung, C.L. Chu, K.W.K. Yeung, W.W. Lu, K.M.C. Cheung, K.D.K. Luk, Surface characteristics, biocompatibility, and mechanical properties of nickel–titanium plasma-implanted with nitrogen at different implantation voltages, J. Biomed. Mater. Res. A 82A (2007) 469–478.